Scientific Research Publishing

Open Journal of Applied Sciences, 2019, 9, 702-709
https://www.scirp.org/journal/ojapps
ISSN Online: 2165-3925
ISSN Print: 2165-3917

The Effect of Mg^{2+} Substitution with Li^{1+} on Structural and Optical Properties of $Zn_{0.5}Li_{2x}Mg_{0.5-x}Fe_2O_4$ Nanoparticles

N. A. Elthair[1,2], Yousef A. Alsabah[1,3*], Eltayeb M. Mustafa[1], Abdelrahman A. Elbadawi[1,4], Abdal Sakhi. Suliman[1]

[1]Department of Physics, Faculty of Science and Technology, Al Neelain University, Khartoum, Sudan
[2]Department of Physics, Faculty of Science, Jazan University, Jazan, KSA
[3]Department of Physics, Faculty of Education and Applied Science, Hajjah University, Hajjah, Yemen
[4]Faculty of Basic Studies, Future University, Khartoum, Sudan
Email: *y.a.alsabah@gmail.com

How to cite this paper: Elthair, N.A., Alsabah, Y.A., Mustafa, E.M., Elbadawi, A.A. and Suliman, A.S. (2019) The Effect of Mg^{2+} Substitution with Li^{1+} on Structural and Optical Properties of $Zn_{0.5}Li_{2x}Mg_{0.5-x}Fe_2O_4$ Nanoparticles. *Open Journal of Applied Sciences*, **9**, 702-709.
https://doi.org/10.4236/ojapps.2019.99057

Received: July 31, 2019
Accepted: September 17, 2019
Published: September 20, 2019

Abstract

Nanoferrite materials had been synthesized to produce new alternate substance for reducing the rare or high cost of industrial materials. In this work, the $Zn_{0.5}Mg_{0.5-x}Li_{2x}Fe_2O_4$ nanoferrite (x = 0.00, 0.10, 0.20, 0.30 and 0.40) was prepared by co-precipitation approach. Structural and optical properties were investigated for the $Zn_{0.5}Mg_{0.5-x}Li_{2x}Fe_2O_4$ series by X-ray diffraction (XRD), Fourier transforms infrared (FTIR) and ultraviolet-visible (UV-Vis) spectroscopies. The XRD data showed that all samples of $Zn_{0.5}Mg_{0.5-x}Li_{2x}Fe_2O_4$ series possess a cubic spinel with a space group (Fd-3m) structure and crystallite size decreased from 116 to 96 nm with a doping ratio. Lattice parameter founded to increases with Li^{1+} ratio that result in the larger ionic radius of the Li^{1+} cation. FTIR result verified the formation of spinel structure by appearance of the absorption bands around 420, 580 cm^{-1}. The energy band gap computed for $Zn_{0.5}Mg_{0.5-x}Li_{2x}Fe_2O_4$ samples and it founded in the range of 3.28 - 3.12eV.

Keywords

Crystal Structure, FTIR, Zn-Li Nanoferrite, XRD, Uv.vis, Zn-Li Nanoparticles

1. Introduction

Particles in the size range of 1 - 100 nm possess novel physical and chemical properties as a result of quantum confinement and surface effects that may find many important applications [1] [2] [3]. Ferrites nanoparticles have the AB_2O_4

formula, where A and B are as transition metals cations, usually including iron [4] [5]. Ferrites have known ferromagnetic materials consisting of ferromagnetic oxides consequently, they are insulating materials. Ferrites nanoparticles are used widely in high-frequency applications [6]. however the Nanoferrite materials are found to use in different physical, chemical and medicine fields, such as semiconductor $CoFe_2O_4$ nanoparticles [7], $ZnFe_2O_4$, $NiFe_2O_4$ in solar cell [8], magnetic resonance $MnFe_2O_4$ [9], microwave $Cd_xCo_{1-x}Fe_2O_4$ (x = 0.0, 0.2, 0.35, 0.5) [10] and biomedical $ZnFe_2O_4$ [11]. In the engineering material science field, ferrite nanoparticles are a unique substance from atoms, and molecules, to build ceramics, or devices [12]. Nano-Ferrites character makes it an ideal candidate for a technical field such as catalysis, sensors and pigments [13]. All ferrite nanoparticles properties are dependent on the cations nature, charges and their distribution through the tetrahedral (A) and octahedral (B) sites [14]. Different preparation methods have been followed to accomplish nanoferrite particles such as solid-state reaction method [15] [16], hydrothermal method [17], sol-gel method [18], co-precipitation route [19], and Chemical combustion route [20]. The chemical co-precipitation route could be the most synthesized method for Mg, Co and Zn Nano-ferrite. It is not very complicated and controlled over crystal structure and extra characters of Substance [21]. A lot of scholars used the co-precipitation route to synthesize nanoferrite materials because the co-precipitation way is a very simple, quick and low-cost method for synthesis, whereas, the nanoparticles that are consequential from co-precipitation are very harmonious [22] [23]. Among those, Kumar *et al.* [24] used a co-precipitation route to synthesize $CoFe_{2-x}GdO_4$. In this work, $Zn_{0.5}Li_{2x}Mg_{0.5-x}Fe_2O_4$ nanoferrite where (x = 0.0, 0.1, 0.2, 0.3 and 0.4) will be synthesized using co-precipitation methods. X-ray diffraction (XRD) and Fourier Transform Infrared Spectroscopy (FTIR) are used to investigate the structure of B-site substituted magnesium Nano ferrites and to determine the crystal structure of the samples. Ultraviolet-visible spectrometer (UV) is used to investigate the optical properties of crystalline nanoparticles.

2. Material and Method

$Zn_{0.5}Mg_{0.5-x}Li_{2x}Fe_2O_4$ nanoparticles samples (x = 0.00, 0.10, 0.20, 0.30 and 0.40) were synthesized by use the co-precipitation route. The raw stoichiometric materials are $FeCl_3$, $MgCl_2{\cdot}6H_2O$, $LiCl{\cdot}H_2O$, $ZnCl_2$ with high pure, NaOH was used to found the required solutions with required molarities. Firstly, the solution of $MgCl_2{\cdot}6H_2O$ 0.2 M (25 ml), $ZnCl_2$ and $FeCl_3$ 0.4 M (25 ml) mixed, next, slowly added of NaOH solution with stirring to obtain a mixture of pH 11 - 12. The colloid solution kept in a water bath at 80˚C for 1.5 hrs to the removal of $NaCl_2$ and H_2O from the powder. The produced powder washed by deionized water until the filtrate had a pH 7. Then the samples were dried and grinned to absolute powder and annealed to 450˚C for 6 hrs in temperature-controlled muffle furnace Vulcan A-550 at a heating rate 10˚C/min. The XRD analysis was carried

out to confirm the purity of the synthesized materials using shimadzu 6000. X-ray diffract meter with Cu-kα radiation of a wavelength λ = 1.5406Å source. FTIR measurements were performed using (Mattson, model 960 m 0016) spectra, while the absorption of a solution with different concentrations was calculated using UV min 1240 spectrometer shimadzu.

3. Results and Discussion

3.1. XRD Result

The crystal structure of samples studied using a Philips PW1700 X-ray diffract meter (operated at 40 kV and current of 30 mA) and the XRD data of all samples were collected between 10O and 80O with 0.06 C/s speed of using Cu Kα radiation with λ = 1.5418 Å. The representative XRD charts of all five $Zn_{0.5}L_{i2x}Mg_{0.5-x}F_{e2}O_4$ samples as shown in **Figure 1**. The XRD data was displayed in **Figure 1** for all powders of $Zn_{0.5}Li_{2x}Mg_{0.5-x}Fe_2O_4$ samples. All crystallites with cubic crystal structure with the Fd-3 m space group [6] [25] [26]. **Table 1** showed the XRD parameters of $Zn_{0.5}Li_{2x}Mg_{0.5-x}Fe_2O_4$ nanopowder, also it described the relation between the rated molar of lithium concentration and structure parameters of samples, that noticed the increase of lattice parameter(a) from 8.379 to 8.408 Å of a sample by increasing the molar of lithium cations, whereas Li^{1+} ionic radius is less than Mg^{2+} cations radii. The crystallite size of samples was calculated by Debye-Scherrer equation [15] [16].

$$D = \frac{k\lambda}{\beta \cos\theta}, \tag{1}$$

That result showed that the samples were crystallite in the nanoscale and that decreased from 116 to 96 nm for series with substitution increasing of Mg^{2+} with Li^{1+} cations.

3.2. FTIR Result

The infrared spectra of synthesized nanoferrite powders were recorded by Mattson Fourier Transform Infrared Spectrophotometer in the range of 400 to 4000 which shown in **Figure 2**. In the present study, the absorption bands are found to be around 420, 580, 1111, 1380 and 1635 cm^{-1}, respectively for all the compositions. The transmittance bands within these specific limits reveal the formation of a single-phase spinel structure having two sub-lattices tetrahedral (A) site and octahedral (B) site. The 420 cm^{-1} band due to the vibrational band of a metal ion at a tetrahedral site with oxygen ions [27]. The band around 582 is caused by the metal-oxygen vibration in the tetrahedral sides. This difference in the spectral positions is due to the different values of metal ion-distances for octahedral and tetrahedral sites. The band around 1111 is due to C-C stretch and C-C-H bending. The 1375 band is associated with the O-H bending vibration. The band around 1639 is due to C=C stretching. The 2621 band is due to the stretching mode of (H-O-H) vibration mode of free or absorbed water which implies that the hydroxyl groups are retained in ferrites [28] [29].

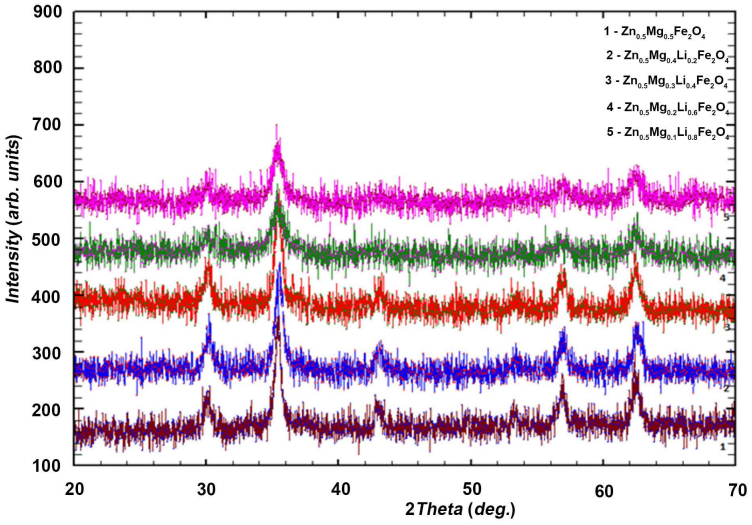

Figure 1. XRD spectrum of $Zn_{0.5}Li_{2x}Mg_{0.5-x}Fe_2O_4$ series.

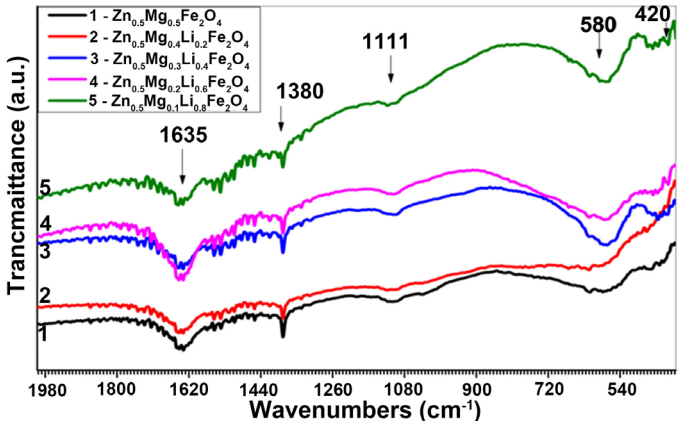

Figure 2. The Fourier Transform Infrared Spectrophotometer of $Zn_{0.5}Li_{2x}Mg_{0.5-x}Fe_2O_4$ samples.

Table 1. The crystal structure parameters of $Zn_{0.5}Li_{2x}Mg_{0.5-x}Fe_2O_4$ samples.

Sample	Crystal Structure	x-ratio of doping	A = b = c (Å)	$\alpha = \beta = \gamma$	Unit cell volume (Å^3)	Density	D (nm)
$Zn_{0.5}Mg_{0.5}Fe_2O_4$	Cubic (Fd-3m)	0.0	8.379	90	588.27	5.055	116
$Zn_{0.5}Li_{0.2}Mg_{0.4}Fe_2O_4$		0.1	8.385	90	589.53	4.310	109
$Zn_{0.5}Li_{0.4}Mg_{0.3}Fe_2O_4$		0.2	8.3873	90	590.02	4.502	111
$Zn_{0.5}Li_{0.6}Mg_{0.2}Fe_2O_4$		0.3	8.396	90	591.9	5.176	97
$Zn_{0.5}Li_{0.8}Mg_{0.1}Fe_2O$		0.4	8.408	90	594.4	5.550	96

3.3. UV. Visible Result

The absorption spectra of was showed in Figure 3 high absorption of all samples noticed at 340 nm. The Tauc plot [30] was used to calculate the bandgap energy Eg of samples. The absorption coefficient α near the band edge in many Nano ferrites shows an exponential upon photon energy usually obeying the relation [25].

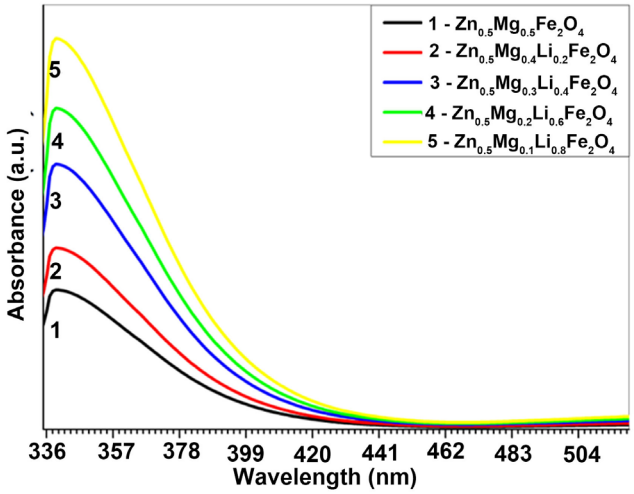

Figure 3. The relation between absorbance and wavelengths of $Zn_{0.5}Li_{2x}Mg_{0.5-x}Fe_2O_4$ samples.

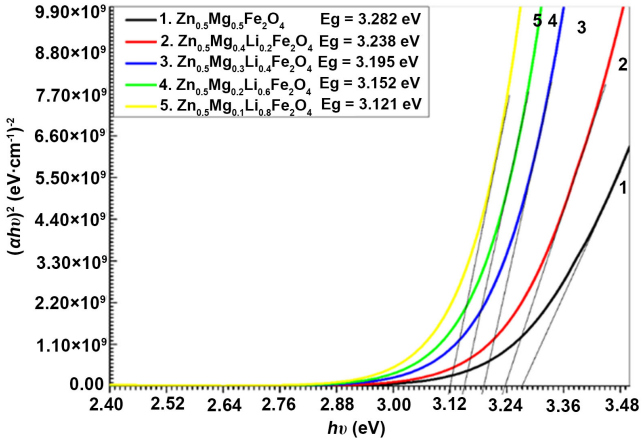

Figure 4. The optical energy bandgab of $Zn_{0.5}Li_{2x}Mg_{0.5-x}Fe_2O_4$ samples.

$$(\alpha h\upsilon) = A(h\upsilon - Eg)^n \tag{2}$$

(α) coefficient of absorption, (A) edge width parameter, Eg is the energy bandgap, (n) is a constant related to the transition degree and ($h\upsilon$) is incident photon energy. **Figure 4** showed the Tauc plot method for samples. The energy band gap is founded in the range 3.28 to 3.12 eV for samples with different concentration (x = 0.0, 0.1, 0.2, 0.3 and 0.4), respectively, it was shoed decreased with substations ratio increasing that may be related to change in the electronic transition levels and occurrence new center transition levels between the conduction and valence bands of molecular.

4. Conclusion

Nanocrystalline, $Zn_{0.5}Mg_{0.5-x}Li_{2x}Fe_2O_4$ Nano ferrites (x = 0.00, 0.10, 0.20, 0.30 and 0.40) samples are successfully prepared by sol-gel approach. The XRD pattern showed a cubic spinel structure for each sample. The lattice parameter is found

an increase from 8.379 to 8.408 Å with Li^{1+} concentration increasing. Also, the crystallite size (D) decreased from 116 to 96 nm with substitution ratio increasing. A Lattice parameter increased with Li^{1+} concentration increasing as a result of the larger ionic radius of the Li^{1+} ion. The FTIR spectrum of the synthesized samples proved the cubic spinel formation. UV-visible spectroscopy showed that the bandgap energy of the samples computed to be 3.28, 3.24, 3.19, 3.15 and 3.12 eV, for Li^{1+} concentration increased for the samples, respectively. This study was limited to the preparation and study of the composition and photometric properties. It is also recommended to study the rest of the physical and chemical properties, especially magnetic properties in order to classify these materials and determine their applications.

Conflicts of Interest

The authors declare no conflicts of interest regarding the publication of this paper.

References

[1] Mirghni, A.A., *et al.* (2015) Synthesis of $Zn_{0.5}CoxMg_{0.5-x}Fe_2O_4$ Nano-Ferrites Using Co-Precipitation Method and Its Structural and Optical Properties. *American Journal of Nano Research and Applications*, **3**, 27-32.

[2] Flores-Acosta, M., *et al.* (2003) Excitonic Absorption of Spherical PbS Nanoparticles in Zeolite A. *Solid State Communications*, **128**, 407-411. https://doi.org/10.1016/j.ssc.2003.09.008

[3] Bognolo, G. (2003) The Use of Surface-Active Agents in the Preparation and Assembly of Quantum-Sized Nanoparticles. *Advances in Colloid and Interface Science*, **106**, 169-181. https://doi.org/10.1016/j.cis.2003.07.002

[4] Pardavi-Horvath, M. (2000) Microwave Applications of Soft Ferrites. *Journal of Magnetism and Magnetic Materials*, **215**, 171-183. https://doi.org/10.1016/S0304-8853(00)00106-2

[5] Spaldin, N.A. (2010) Magnetic Materials: Fundamentals and Applications. Cambridge University Press, Cambridge. https://doi.org/10.1017/CBO9780511781599

[6] Deraz, N. and Abd-Elkader, O.H. (2015) Structural, Morphological and Magnetic Properties of $Zn_{0.5}Mg_{0.5}Fe_2O_4$ as Anticorrosion Pigment. *International Journal of Electrochemical Science*, **10**, 7138-7146.

[7] Kumar, S., Munjal, S. and Khare, N. (2017) Metal-Semiconductor Transition and Seebeck Inversion in $CoFe_2O_4$ Nanoparticles. *Journal of Physics and Chemistry of Solids*, **105**, 86-89. https://doi.org/10.1016/j.jpcs.2017.02.003

[8] Kovalenko, A., *et al.* (2016) Towards Improved Efficiency of Bulk-Heterojunction Solar Cells Using Various Spinel Ferrite Magnetic Nanoparticles. *Organic Electronics*, **39**, 118-126. https://doi.org/10.1016/j.orgel.2016.09.033

[9] Zhang, H., *et al.* (2017) Ultrasmall Ferrite Nanoparticles Synthesized via Dynamic Simultaneous Thermal Decomposition for High-Performance and Multifunctional T1 Magnetic Resonance Imaging Contrast Agent. *ACS Nano*, **11**, 3614-3631. https://doi.org/10.1021/acsnano.6b07684

[10] Ahmad, R., *et al.* (2016) Improved Electrical Properties of Cadmium Substituted Cobalt Ferrites Nano-Particles for Microwave Application. *Journal of Magnetism*

and Magnetic Materials, **405**, 28-35. https://doi.org/10.1016/j.jmmm.2015.12.019

[11] Hoque, S.M., *et al.* (2016) Synthesis and Characterization of $ZnFe_2O_4$ Nanoparticles and Its Biomedical Applications. *Materials Letters*, **162**, 60-63. https://doi.org/10.1016/j.matlet.2015.09.066

[12] Pulišová, P., *et al.* (2013) Structure and Magnetic Properties of Co and Ni Nano-Ferrites Prepared by a Two Step Direct Microemulsions Synthesis. *Journal of Magnetism and Magnetic Materials*, **341**, 93-99. https://doi.org/10.1016/j.jmmm.2013.04.003

[13] Ganjkhanlou, Y., *et al.* (2014) Application of Image Analysis in the Characterization of Electrospun Nanofibers. *Iranian Journal of Chemistry and Chemical Engineering*, **33**, 37-45.

[14] Nikumbh, A., *et al.* (2014) Structural, Electrical, Magnetic and Dielectric Properties of Rare-Earth Substituted Cobalt Ferrites Nanoparticles Synthesized by the Co-Precipitation Method. *Journal of Magnetism and Magnetic Materials*, **355**, 201-209. https://doi.org/10.1016/j.jmmm.2013.11.052

[15] Alsabah, Y.A., *et al.* (2017) Influence of Zn^{2+} and Ni^{2+} Cations on the Structural and Optical Properties of $Ba_2Zn_{1-x}NixWO_6$ ($0 \leq x \leq 1$) Tungsten Double Perovskites. *Journal of Alloys and Compounds*, **701**, 797-805. https://doi.org/10.1016/j.jallcom.2017.01.203

[16] Alsabah, Y.A., *et al.* (2017) Synthesis and Study of the Effect of Ba^{2+} Cations Substitution with Sr^{2+} Cations on Structural and Optical Properties of $Ba_{2-x}SrxZnWO_6$ Double Perovskite Oxides (x = 0.00, 0.25, 0.50, 0.75, 1.00). *Materials*, **10**, 469. https://doi.org/10.3390/ma10050469

[17] Khorrami, S.A. and Manuchehri, Q.S. (2013) Magnetic Properties of Cobalt Ferrite Synthesized by Hydrothermal and Co-Precipitation Methods: A Comparative Study. *Journal of Applied Chemical Research*, **7**, 15-23.

[18] Huixia, F., *et al.* (2014) Preparation and Characterization of the Cobalt Ferrite Nano-Particles by Reverse Coprecipitation. *Journal of Magnetism and Magnetic Materials*, **356**, 68-72. https://doi.org/10.1016/j.jmmm.2013.12.033

[19] Zhang, Y., *et al.* (2010) Composition and Magnetic Properties of Cobalt Ferrite Nano-Particles Prepared by the Co-Precipitation Method. *Journal of Magnetism and Magnetic Materials*, **322**, 3470-3475. https://doi.org/10.1016/j.jmmm.2010.06.047

[20] Kambale, R., *et al.* (2010) Structural and Magnetic Properties of $Co_{1-x}Mn_xFe_2O_4$ ($0 \leq x \leq 0.4$) Spinel Ferrites Synthesized by Combustion Route. *Journal of Alloys and Compounds*, **490**, 568-571. https://doi.org/10.1016/j.jallcom.2009.10.082

[21] Azhagushanmugam, S., Suriyanarayanan, N. and Jayaprakash, R. (2014) Magnetic Properties of Zinc-Substituted Cobalt Ferric Oxide Nanoparticles: Correlation with Annealing Temperature and Particle Size. *Materials Science in Semiconductor Processing*, **21**, 33-37. https://doi.org/10.1016/j.mssp.2014.01.023

[22] Rajaeiyan, A. and Bagheri-Mohagheghi, M.M. (2013) Comparison of Sol-Gel and Co-Precipitation Methods on the Structural Properties and Phase Transformation of γ and α-Al2O3 Nanoparticles. *Advances in Manufacturing*, **1**, 176-182. https://doi.org/10.1007/s40436-013-0018-1

[23] de Mello, L.B., *et al.* (2019) Co-Precipitation Synthesis of (Zn-Mn)-Co-Doped Magnetite Nanoparticles and Their Application in Magnetic Hyperthermia. *Journal of Alloys and Compounds*, **779**, 698-705. https://doi.org/10.1016/j.jallcom.2018.11.280

[24] Chand, J., *et al.* (2011) Structural, Electric and Dielectric Properties of $MgFe_2O_4$ Ferrite Processed by Solid State Reaction Technique. *International Journal of Theoretical and Applied Science*, **3**, 8-9.

[25] Ali, B.M., *et al.* (2018) Effect of Cu^{2+} Doping on Structural and Optical Properties of Synthetic $Zn_{0.5}Cu_xMg_{0.5-x}Fe_2O_4$ (x = 0.0, 0.1, 0.2, 0.3, 0.4) Nano-Ferrites. *Advances in Nanoparticles*, **7**, 1.

[26] Bushkova, V. (2015) Synthesis and Study of the Properties of Nanoferrites Obtained by the Sol-Gel Method with Participation of Auto-Combustion. *Journal of Nano and Electronic Physics*, **7**, Article ID: 01023.

[27] Rahman, S., *et al.* (2013) Structural and Magnetic Properties of ZnMg-Ferrite Nanoparticles Prepared Using the Co-Precipitation Method. *Ceramics International*, **39**, 5235-5239. https://doi.org/10.1016/j.ceramint.2012.12.023

[28] King, R.B. (2005) Encyclopedia of Inorganic Chemistry. Vol. 1, Wiley, Hoboken.

[29] Akhtar, F. and Podder, J. (2011) Structural, Optical, Electrical and Thermal Characterizations of Pure and L-Alanine Doped Ammonium Dihydrogen Phosphate Crystals. *Journal of Crystallization Process and Technology*, **1**, 18. https://doi.org/10.4236/jcpt.2011.12004

[30] Chattopadhyay, S., *et al.* (2019) Correlated Quartic Variation of Band Gap and NBE Energy in Sol-Gel Derived $Zn_{1-x}Co_xO$ Nanoparticles. *Materials Chemistry and Physics*, **227**, 236-241. https://doi.org/10.1016/j.matchemphys.2019.02.003